

# The Properties of a Black Hole-Neutron Star Merger Candidate

James M. Lattimer<sup>1</sup>

<sup>1</sup> *Department of Physics and Astronomy, Stony Brook University, Stony Brook, NY 11794-3800, USA*

The LIGO/Virgo Consortium (LVC) released a preliminary announcement of a candidate gravitational wave signal, S190426c, that could have arisen from a black hole-neutron star merger. As the first such candidate system, its properties such as masses and spin are of great interest. Although LVC policy prohibits disclosure of these properties in preliminary announcements, LVC does release the estimated probabilities that this system is in specific categories, such as binary neutron star, binary black hole and black hole-neutron star. LVC also releases information concerning relative signal strength, distance, and the probability that ejected mass or a remnant disc survived the merger. In the case of events with a finite probability of being in more than one category, such as is likely to occur with a black hole-neutron star merger, it is shown how to estimate the masses of the components and the spin of the black hole. This technique is applied to the source S190426c.

## INTRODUCTION

On April 26, 2019 The LIGO/Virgo Consortium (LVC) observed gravitational waves from a possible compact object coalescence, S190426c [1, 2] that could be the first observed black hole-neutron star (BHNS) system. GCN circular 24237 [1] reported a false alarm probability of  $1.9\text{e-}08$  Hz or once every 1 year, 7 months, which indicates a moderately low signal-to-noise (S/N) ratio, supported by the 14% estimated probability of being a terrestrial anomaly. Initially, the system was assigned a probability  $p_{\text{BNS}} = 57\%$  of being a binary neutron star (BNS),  $p_{\text{BHNS}} = 15\%$  of being a BHNS system,  $p_{\text{gap}} = 28\%$  of being a MassGap system (henceforth called 'gap'), and  $p_{\text{BBH}} < 1\%$  of being a binary black hole system (BBH), assuming it is cosmic in origin. These classifications are based on the convention that component masses less than  $3M_{\odot}$  are neutron stars and those greater than  $5M_{\odot}$  are black holes. Systems with one or two components in the gap between  $3M_{\odot}$  and  $5M_{\odot}$  are classified as gap. In addition, it was reported that the probabilities that mass existed outside of the compact remnant at least briefly after the coalescence, HasRemnant (henceforth  $p_d$ ), and that at least one component was a neutron star, HasNS (henceforth  $p_{\text{NS}}$ ), were both  $> 99\%$ . The source classification probabilities, but not the source distance, false alarm rate, terrestrial anomaly probability, and  $p_{\text{NS}}$ , were later revised in GCN circular 24144 [2] to be  $p_{\text{BNS}} = 15\%$ ,  $p_{\text{BHNS}} = 60\%$ ,  $p_{\text{gap}} = 25\%$  and  $p_{\text{BBH}} < 1\%$ , assuming the source is cosmic in origin. In addition,  $p_d$  was revised to 72%, indicating that mass ejection is considered likely. As originally proposed in Ref. [3], some BHNS mergers could result in mass ejection leading to the synthesis of r-process nuclei [4, 5], and an optical signature [6, 7]. It is therefore of great interest to understand more about this system, including its component masses.

It should be noted that the neutron star maximum mass is undoubtedly less than about  $3M_{\odot}$  due to causality, so that gap objects are presumably black holes. Therefore, gap systems are, in conventional notation, either BHNS or BBH systems. Since the system has greater than 99% chance of containing one neutron star, the reported probabilities indicate that there is actually an 85% chance of this being a BHNS system.

In principle, the system's chirp mass  $\mathcal{M} = (M_1 M_2)^{3/5} / (M_1 + M_2)^{1/5}$  ought to have been determined to relatively high precision even in the case of a BHNS merger with a relatively low S/N ratio. With a S/N ratio approximately 3, extrapolating the results of Ref. [8] indicates  $\Delta\mathcal{M}/\mathcal{M} \sim 0.003$ . However, in all likelihood, the binary mass ratio  $q = M_1/M_2 \geq 1$  and component spins were determined relatively poorly; a similar extrapolation indicates  $\Delta\eta/\eta \sim 0.5$  where  $\eta = q/(1+q)^2$  is the symmetric mass ratio. Unfortunately, current collaboration policy forbids the release of  $\mathcal{M}$ ,  $q$  and spin estimates or their uncertainties. Therefore, it is not possible to learn the likely source masses or spins until publication of a peer-reviewed article, which may not occur for several months following a detection. Fortunately, it is possible to estimate the system masses and black hole spin from the information released in the GCN circulars with a few straightforward assumptions.

## METHOD

The case of BHNS mergers is especially interesting, because at least three classification categories likely then have finite probabilities which provides additional information compared to BNS or BBH events. It is convenient to examine this problem, not in  $M_1 - M_2$  space, but in  $\mathcal{M} - q$  or  $\mathcal{M} - \eta$  space, because  $\mathcal{M}$  presumably has a very small uncertainty. However, due to their expected large uncertainties,  $q$  or  $\eta$  are not suitable variables given their ranges  $q \in [1, \infty]$  and  $\eta \in [0, 1/4]$  for which Gaussian probability distribution with any finite uncertainty  $\sigma_q$  or  $\sigma_\eta$  will extend into the non-physical regions  $q < 1$  or  $\eta > 1/4$ . It is convenient to employ the alternate variable  $\bar{q} = \ln(q - 1)$  which has the range  $\bar{q} \in [-\infty, \infty]$ . Note that  $\bar{q} = [-1, 0, 1]$  corresponds to  $q = [1.37, 2, 3.72]$ . We will refer to the uncertainty in  $\bar{q}$  by  $\sigma_{\bar{q}}$  for notational simplicity. Fig. 1 shows classifications in  $\mathcal{M} - \bar{q}$  space, together with some  $M_1$  and  $M_2$  contours.

Given measurements  $\mathcal{M}_0 \pm \sigma_{\mathcal{M}}$  and  $\bar{q}_0 \pm \sigma_{\bar{q}}$ , we take the probability density of an event having  $\mathcal{M}$  and  $\bar{q}$  to be

$$\frac{d^2 p}{d\mathcal{M} d\bar{q}} = A \exp \left[ -\frac{(\mathcal{M} - \mathcal{M}_0)^2}{2\sigma_{\mathcal{M}}^2} - \frac{(\bar{q} - \bar{q}_0)^2}{2\sigma_{\bar{q}}^2} \right] \quad (1)$$

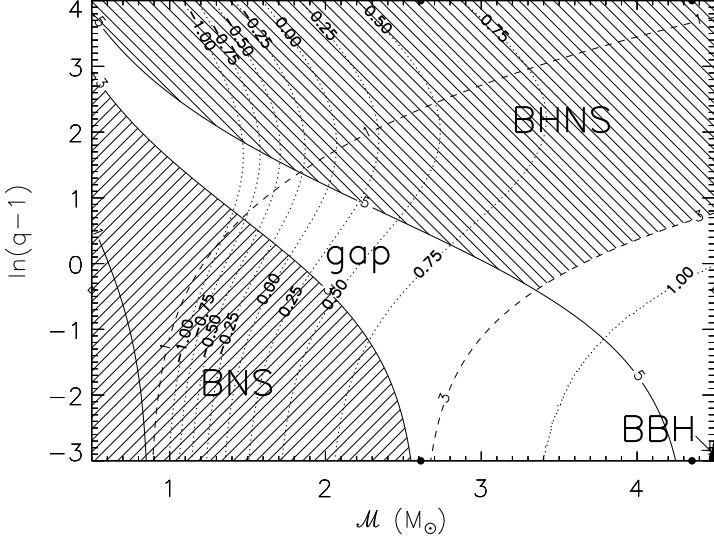


FIG. 1. Compact binary classifications in the  $\mathcal{M} - \bar{q}$  plane. BNS and BHNS regions are hatched, the gap region is unshaded, and the BBH region is solid. Labelled contours of  $M_1(M_2)$  in  $M_\odot$  are shown as solid (dashed) curves. Dotted contours are the boundaries  $M_d = 0$  labelled for various values of black hole spin parameter  $\chi$ . Filled points show the maximum (minimum)  $\mathcal{M}$  values for BNS (BBH) systems. Diamonds show the minimum  $\bar{q}$  value for BHNS systems.

where  $A = (2\pi\sqrt{\sigma_{\mathcal{M}}\sigma_q})^{-1}$ . It is assumed that the uncertainties in  $\mathcal{M}$  and  $\bar{q}$  are uncorrelated. One expects that  $\sigma_{\mathcal{M}}$  will be very small, possibly of order a few hundredths of a solar mass or less, while  $\sigma_q$  will be large, of order unity or larger. Therefore, results should be insensitive to  $\sigma_{\mathcal{M}}$ .

For given values of  $\mathcal{M}_0$  and  $\bar{q}_0$ , the integration of the probability density over all values of  $\mathcal{M}$  and  $\bar{q}$  corresponding to the BNS, gap, BHNS and BBH regions yields the probabilities  $p_{\text{BNS}}, p_{\text{gap}}, p_{\text{BHNS}}$  and  $p_{\text{BBH}}$ , respectively, which will add to unity. Each of these probabilities are therefore functions of four variables  $[\mathcal{M}, \sigma_{\mathcal{M}}, \bar{q}, \sigma_q]$ . A particular choice of  $\sigma_{\mathcal{M}}$  and  $\sigma_q$  then allows probability contours to be drawn in  $\mathcal{M} - \bar{q}$  space. However, because  $\sigma_{\mathcal{M}}$  is relatively small, these contours are insensitive to  $\sigma_{\mathcal{M}}$  and depend primarily on  $\sigma_q$ . Fig. 2 shows these probability contours for  $\sigma_{\mathcal{M}} = 0.01\mathcal{M}$  for the cases  $\sigma_q = [1.0, 2.5]$ .

Realistically, neutron stars have a minimum mass around  $1M_\odot$ , but the LVC algorithm doesn't consider this minimum when assigning classification probabilities. Therefore, there is no lower bound to  $\mathcal{M}$  for BNS although there is an upper bound. Because  $\sigma_{\mathcal{M}}$  is small,  $p_{\text{BNS}} > 0.01$  requires  $\mathcal{M}/M_\odot < 3/2^{1/5} = 2.612$ . Similarly,  $p_{\text{BBH}} > 0.01$  requires  $\mathcal{M}/M_\odot > 5/2^{1/5} = 4.353$ . There are no  $\mathcal{M}$  bounds for gap or BHNS events with finite probabilities. But a minimum value  $q > 5/3$  is required for  $p_{\text{BHNS}} \gtrsim 0.01$ .

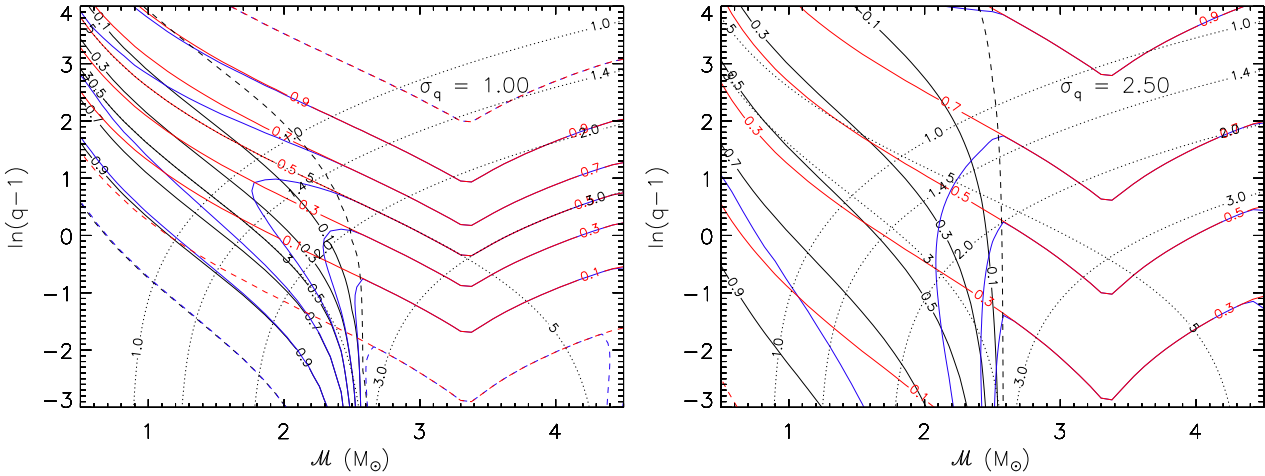


FIG. 2. Classification probability contours for two values of  $\sigma_q$ . In all cases,  $\sigma_{\mathcal{M}} = 0.01\mathcal{M}$ . Solid red (black) contours show probabilities for BHNS (BNS) systems; blue solid contours show gap probabilities. Only BHNS and BNS contours are labelled. Dashed contours indicate probabilities of 0.01 or 0.99 for each class. Dotted curves are contours of  $M_1(3M_\odot, 5M_\odot)$  and  $M_2(M_\odot, 1.4M_\odot, 2M_\odot, 3M_\odot)$ .

For systems with a finite chance of being a BNS binary,  $p_{\text{NS}}$  is always greater than 0.99 and therefore provides no additional information to constrain  $\mathcal{M}$  and  $\bar{q}$ . For small  $\bar{q}$ , the  $p_{\text{NS}} = 0.99$  contour lies close to the limiting curve for the smaller component to be a neutron star, i.e.,  $M_2 = 3M_\odot$  (see

Fig. 3). But for larger values of  $q$ , especially for large  $\sigma_q$ , this contour becomes more vertical than the  $M_2 = 3M_\odot$  contour. For  $\bar{q} \gtrsim 0$ , the  $p_{\text{NS}} = 0.99$  contour always lies to the right of that for  $p_{\text{BNS}} = 0.01$ .

Another quantity provided [2] is the probability,  $p_d$ , of hav-

ing disrupted material outside the merged object. This, together with the determination of  $\mathcal{M}$  and  $\bar{q}$  with the above method, allows an estimate of the black hole spin by using an analytic model for the mass  $M_d$  of disrupted material [9, 10]. The same model, which has three free parameters and was fit to relativistic hydrodynamical results, was used by LVC to determine  $p_d$  from their inferred values of  $\mathcal{M}$  and  $q$  [11]. It approximates the combined mass,  $M_d$ , of the accretion disk, the tidal tail, and the potential ejecta, remaining outside the black hole a few milliseconds after a BHNS merger, by

$$M_d \simeq M_{\text{b,NS}} \left[ \frac{\alpha'}{\eta^{1/3}} (1 - 2\beta) - \frac{\beta'}{\eta} \hat{R}_{\text{ISCO}} \beta + \gamma' \right], \quad (2)$$

where  $\beta = GM_{\text{NS}}/(R_{\text{NS}}c^2)$  is the neutron star compactness,  $R_{\text{NS}}$  is the neutron star radius,  $M_{\text{b,NS}}$  is the baryon mass of the neutron star, and  $\hat{R}_{\text{ISCO}} = R_{\text{ISCO}}c^2/(GM_{\text{BH}})$ .  $R_{\text{ISCO}}$  is the radius of the innermost stable circular orbit, from which the black hole spin parameter  $\chi$  may be found:

$$\chi = \frac{\sqrt{\hat{R}_{\text{ISCO}}}}{3} \left( 4 - \sqrt{3\hat{R}_{\text{ISCO}} - 2} \right). \quad (3)$$

The model is claimed to be accurate to within a few percent of the mass of the neutron star,  $M_{\text{NS}}$ . The model constants are  $\alpha' \simeq 0.406$ ,  $\beta' \simeq 0.139$ , and  $\gamma' = 0.255$ . LVC have assumed  $R_{\text{NS}} = 15$  km [11]. The boundary of the  $\mathcal{M} - \bar{q}$  plane permitting non-zero  $M_d$ , is then found from

$$\hat{R}_{\text{ISCO}} \simeq (\beta'\beta)^{-1} \left( \alpha'\eta^{2/3}(1 - 2\beta) + \gamma'\eta \right), \quad (4)$$

which contains only two model parameters. The boundaries for various values of  $\chi$  are shown in Fig. 1; the regions to the left of each boundary are where  $M_d > 0$ . It should be noted that values of  $\chi < -1$  and  $\chi > 1$  are possible solutions of Equations (3) and (4). These admittedly unphysical regions are unlikely to be populated by BHNS mergers, as judged by numerical relativity simulations.

The probability  $p_d$  for a given value of  $\chi$  can be determined by integrating  $d^2p/d\mathcal{M}d\bar{q}$  over the region in  $\mathcal{M} - \bar{q}$  space permitting non-zero  $M_d$ . When  $p_d$  is provided, the likely black hole spin is found by observing which  $\chi$  contours corresponding to this value of  $p_d$  pass through the favored  $[\mathcal{M}, \bar{q}]$  region determined by satisfying the  $p_{\text{BNS}}, p_{\text{gap}}$  and  $p_{\text{BHNS}}$  conditions. As is the case for  $\mathcal{M}$  and  $\bar{q}$  themselves, the inferred value of  $\chi$  is insensitive to  $\sigma_{\mathcal{M}}$  and depends mostly on  $\sigma_{\bar{q}}$ .

#### APPLICATION TO S190426C

The event S190426c [2] was reported to have  $p_{\text{BNS}} = 3/20$ ,  $p_{\text{gap}} = 5/20$ ,  $p_{\text{BHNS}} = 12/20$ ,  $p_d = 0.72$ , and  $p_{\text{NS}} > 0.99$  (which is not useful, as previously described). We assume that the classification probabilities are uncertain by  $\pm 0.5/20$ . One can then identify the most likely values of  $\mathcal{M}$  and  $\bar{q}$  by plotting regions defined by  $p_{\text{BNS}} = 0.15 \pm 0.025$ ,

$p_{\text{gap}} = 0.25 \pm 0.025$  and  $p_{\text{BHNS}} = 0.60 \pm 0.025$  and identifying any overlap regions (Fig. 3). It is assumed that  $\sigma_{\mathcal{M}} = 0.01\mathcal{M}$  based on likely expectations for even small S/N events, but in any case these contours are very insensitive to this parameter as long as  $\sigma_{\mathcal{M}} < 0.1\mathcal{M}$ . This insensitivity is not the case for  $\sigma_{\bar{q}}$ , however. Results for selected choices of  $\sigma_{\bar{q}}$  are shown in Fig. 3. For  $\sigma_{\bar{q}} \gtrsim 1.25$ , consistent solutions become possible.

When a consistent solution is possible, a region in  $\mathcal{M} - \bar{q}$  space is outlined. The overall uncertainties are established by combining the size of this region with the assumed values of  $\sigma_{\mathcal{M}}$  and  $\sigma_{\bar{q}}$ . The implied  $\mathcal{M} - \bar{q}$  confidence ellipses are shown in Fig. 3. While the individual masses have large uncertainties because  $\sigma_{\bar{q}}$  is large, the inferred centroids of the black hole mass for those cases where a consistent solution exists is relatively independent of the actual value of  $\sigma_{\bar{q}}$ , and is around  $6M_{\odot}$  (Fig. 4). The neutron star mass, on the other hand, increases progressively up to  $\sim 1.4M_{\odot}$  as  $\sigma_{\bar{q}}$  is increased.

These results suggest the existence in S190426c of a relatively low-mass neutron star. For the smallest values of  $\sigma_{\bar{q}} \simeq 1.25$  for which a consistent solution is possible, the inferred mass, about  $0.25M_{\odot}$ , is less than the minimum possible neutron star mass, about  $1.1M_{\odot}$ , that can be made in core-collapse supernova events [12, 13]. The lowest well-measured neutron star mass, the companion to PSR J0453+1559, is  $1.174 \pm 0.004M_{\odot}$  [14]. The observed BNS population currently consists of 9 systems with well-measured individual masses and 7 systems with well-measured total masses  $M_T$ . Assuming these are sampled from a Gaussian distribution, Ref. [15] obtained a mean mass  $1.33 \pm 0.09M_{\odot}$  from fitting 7 of the 9 systems with well-measured individual masses. Including all 16 systems one finds the nearly identical result,  $1.325 \pm 0.095M_{\odot}$ . The systems for which only the total mass is known can be treated assuming the lower (higher) mass star cannot have a mass greater (less) than  $M_T/2$ , and that the minimum neutron star mass is  $M_{\text{min}} = 1.1M_{\odot}$ , as argued above. Assuming these systems are more likely to be symmetric than highly asymmetric, as observed for other BNS systems, it seems justified to assume that the lower mass component has mass  $M_2$  with a probability proportional to  $M_2 - M_{\text{min}}$  for  $M_{\text{min}} < M_2 < M_T/2$ , and the higher mass component has mass  $M_1$  with a probability proportional to  $M_T - M_{\text{min}} - M_1$  for  $M_T/2 < M_1 < M_T - M_{\text{min}}$ . The 95% confidence bounds for this distribution,  $[1.135M_{\odot}, 1.515M_{\odot}]$ , estimated using twice the standard deviation  $0.095M_{\odot}$ , are indicated in Fig. 3. Values of  $\sigma_{\bar{q}} \gtrsim 2$  then predict a neutron star mass consistent with the observed distribution.

From the value  $p_d = 0.72$ , the inferred black hole spin  $\chi$  values, with uncertainties determined from the size of the overlap region in  $\mathcal{M} - \bar{q}$  space, are shown as a function of  $\sigma_{\bar{q}}$  in Fig. 4, along with inferred ranges of  $\mathcal{M}$ ,  $M_{\text{NS}}$ , and  $M_{\text{BH}}$ . Note that for  $\sigma_{\bar{q}} \lesssim 1.5$ , the minimum  $\chi$  may fall below -1. As this is unphysical, it strongly supports larger values of  $\sigma_{\bar{q}}$ , which is consistent with the results implied by realistic values of  $M_{\text{NS}}$ .

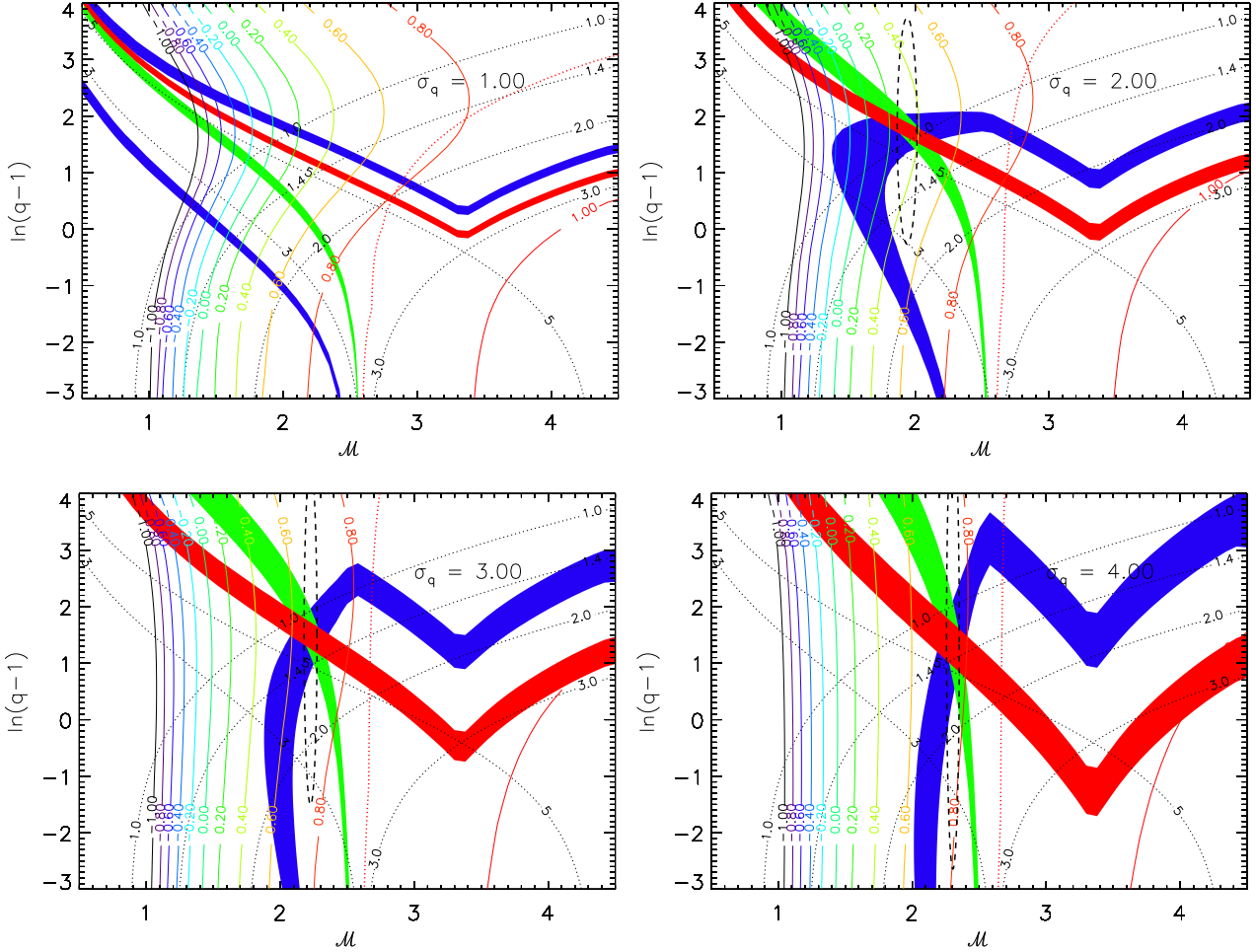


FIG. 3. Probability regions matching those reported by LVC for the possible BHNS event S190426c for four assumed values of  $\sigma_q$ . The green, blue and red regions show where  $p_{\text{NS}} = 0.150 \pm 0.025$ ,  $p_{\text{gap}} = 0.250 \pm 0.025$ , and  $p_{\text{BHNS}} = 0.600 \pm 0.025$ , respectively. Labelled solid contours show the black hole spin parameters  $\chi$  where  $p_d = 0.72$ . The red dotted contour is  $p_{\text{NS}} = 0.01$ . The dashed ellipsoid represents the inferred  $1\sigma$  confidence ellipse consistent with all three probabilities.

## DISCUSSION

It is interesting that, irrespective of assumptions concerning  $\sigma_q$ , we predict that  $M_{\text{BH}} \simeq 6M_{\odot}$ , and, in the case of moderate to large values of  $\sigma_q$ , we find that  $M_{\text{NS}}$  converges to the range expected from observed binary neutron star masses. LVC initially reported that the probability that this event was terrestrial, i.e., that it is spurious, to be 14%, and have not updated that estimate. The fact that we find physically realistic values for  $M_{\text{NS}}$  seems to lend a degree of credulity to the real nature of this event and supports moderate to large values of  $\sigma_q$ , with an inferred mass ratio  $q \sim 4$ . On the other hand, the inferred  $\chi$  values for large  $\sigma_q \gtrsim 3$  approach 0.75. Such rapidly spinning black holes are inconsistent with smaller values inferred from BBH mergers [16]. The mean value of the effective binary spin  $\chi_{\text{eff}} = (M_1\chi_1 + M_2\chi_2)/(M_1 + M_2)$  for the first 10

BBH observed by LVC was  $0.046 \pm 0.052$ . Smaller values of  $\chi \sim 0$  would favor  $1.75 \lesssim \sigma_q \lesssim 2.25$ , suggesting that  $M_{\text{NS}}$  is near the lower end of the range of observed masses.

LVC overestimates the probability of a surviving remnant. As previously noted, LVC assumes a value  $R_{\text{NS}} = 15$  km to estimate  $M_d$  from Equation (2). This radius value is unrealistically large, given evidence from nuclear experiment and theory [17], as well as from the tidal deformations inferred from GW170817 [18, 19]. A more realistic value  $R_{\text{NS}} \simeq 12$  km makes the probability of a surviving disc much less likely since the resulting  $\chi$  contours in Figs. 1 and 3 would be shifted considerably to the left. Changing  $R_{\text{NS}}$  to 12 km would change the condition needed for  $M_d > 0$  from  $\chi > 0.25$  for our suggested solution  $M \simeq 2.3M_{\odot}$  and  $\bar{q} \simeq 1.5$  (see Fig. 1) to  $\chi > 0.60$ . For  $\sigma_q$  in the range 1.75 - 2.25, one then finds the condition  $p_d \gtrsim 0.0$  requires  $\chi \gtrsim 0.5$ , consider-

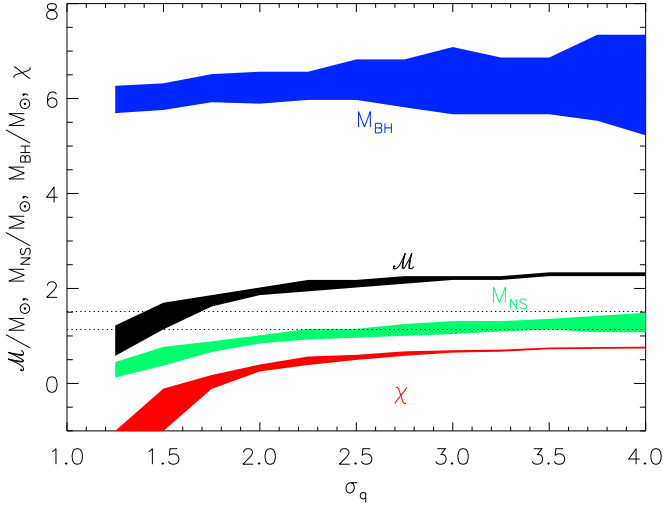


FIG. 4. Inferred  $\mathcal{M}$ ,  $M_{\text{NS}}$ ,  $M_{\text{BH}}$  and  $\chi$  for S190426c as functions of  $\sigma_q$ . The dotted lines indicate the 95% confidence interval determined from the observed binary neutron star mass distribution (see text).

ably larger than our favored value near zero. In other words, the use of a more realistic neutron star radius together with our inferred  $\mathcal{M}$  and  $\bar{q}$  values implies that the formation of a remnant disc is much less likely than announced. It is thought that if a disc cannot form, tidal or wind ejection of matter is also unlikely, and the resulting synthesis of radioactive heavy nuclei and subsequent optical emission is not possible. This would be consistent with the apparent failure to observe an electromagnetic counterpart.

#### ACKNOWLEDGEMENTS

I thank Will Farr for helpful discussions. This work was supported by DOE Award DE-FG02-87ER40317.

- [1] LIGO Scientific Collaboration and the Virgo Collaboration, GRB Coordinates Network, Circular Service **24168** (2019a).
- [2] LIGO Scientific Collaboration and the Virgo Collaboration, GRB Coordinates Network, Circular Service **24411** (2019b).
- [3] J. M. Lattimer and D. N. Schramm, Ap. J. Lett. **192**, L145 (1974).
- [4] J. M. Lattimer and D. N. Schramm, Ap. J. **210**, 549 (1976).
- [5] J. M. Lattimer, F. Mackie, D. G. Ravenhall, and D. N. Schramm, Ap. J. **213**, 225 (1977).
- [6] L.-X. Li and B. Paczyński, Ap. J. Lett. **507**, L59 (1998), arXiv:astro-ph/9807272 [astro-ph].
- [7] B. D. Metzger, G. Martínez-Pinedo, S. Darbha, E. Quataert, A. Arcones, D. Kasen, R. Thomas, P. Nugent, I. V. Panov, and N. T. Zinner, MNRAS **406**, 2650 (2010), arXiv:1001.5029 [astro-ph.HE].
- [8] B. D. Lackey, *The neutron-star equation of state and gravitational waves from compact binaries*, Ph.D. thesis, The University of Wisconsin - Milwaukee (2012).
- [9] F. Foucart, Phys. Rev. D **86**, 124007 (2012), arXiv:1207.6304 [astro-ph.HE].
- [10] F. Foucart, T. Hinderer, and S. Nissanke, Phys. Rev. D **98**, 081501 (2018), arXiv:1807.00011 [astro-ph.HE].
- [11] W. Farr, private communication (2019).
- [12] K. Strobel, C. Schaab, and M. K. Weigel, Ast. & Ap. **350**, 497 (1999), arXiv:astro-ph/9908132 [astro-ph].
- [13] Y. Suwa, T. Yoshida, M. Shibata, H. Umeda, and K. Takahashi, MNRAS **481**, 3305 (2018), arXiv:1808.02328 [astro-ph.HE].
- [14] J. G. Martinez, K. Stovall, P. C. C. Freire, J. S. Deneva, F. A. Jenet, M. A. McLaughlin, M. Bagchi, S. D. Bates, and A. Riodolfi, Ap. J. **812**, 143 (2015), arXiv:1509.08805 [astro-ph.HE].
- [15] F. Özel and P. Freire, Ann. Rev. Ast. Ap. **54**, 401 (2016), arXiv:1603.02698 [astro-ph.HE].
- [16] S. S. Bavera, T. Fragos, Y. Qin, E. Zapartas, C. J. Neijssel, I. Mandel, A. Batta, S. M. Gaebel, C. Kimball, and S. Stevenson, arXiv e-prints, arXiv:1906.12257 (2019), arXiv:1906.12257 [astro-ph.HE].
- [17] J. M. Lattimer and Y. Lim, Ap. J. **771**, 51 (2013), arXiv:1203.4286 [nucl-th].
- [18] S. De, D. Finstad, J. M. Lattimer, D. A. Brown, E. Berger, and C. M. Biwer, Phys. Rev. Lett. **121**, 091102 (2018), arXiv:1804.08583 [astro-ph.HE].
- [19] B. P. Abbott, LIGO Scientific Collaboration, and the Virgo Collaboration, Phys. Rev. Lett. **121**, 161101 (2018), arXiv:1805.11581 [gr-qc].